

INFLUENCE OF ANCHOR INCLINATION AND LENGTH ON THE STABILITY OF EXCAVATED ROADBED SLOPES REINFORCED WITH ANCHORS

Vo Hai Lang¹, Chau Truong Linh^{1*}, Hoang Phuong Hoa¹, Tran Thanh Quang²,
Vu Trong Quyen¹, Ha Ngoc Thang¹

¹The University of Danang - University of Science and Technology, Vietnam

²The University of Danang - University of Technology and Education, Vietnam

*Corresponding author: ctlinh@dut.udn.vn

(Received: May 03, 2025; Revised: June 20, 2025; Accepted: June 22, 2025)

DOI: 10.31130/ud-jst.2025.23(10C).669E

Abstract - This study investigates the influence of anchor angle and anchor length on the stability of roadbed slopes. The study is based on a cut slope with height $H=21$ meters, divided into three levels and considering three different geological configurations. Two slope ratios are analyzed: 1:0.5 and 1:0.75. Conventional steel anchors are used and the theoretical basis is the numerical method. The stability of the slope is analyzed using FLAC software with the theoretical basis of the finite difference method. The study determines the optimal anchor angle by evaluating the range from 20°, 25°, 30°, ..., 50°. The study also compares two reinforcement scenarios: 9 anchors with a length of 8 meters and 6 anchors with a length of 10 meters, to determine the most reasonable configuration. In addition, the critical sliding surface corresponding to each optimal anchor angle is determined.

Key words - Design; Roadbed; Steel anchor; Optimal anchor angle; Optimal anchor length

1. Introduction

Currently, under the increasing impact of climate change, extreme weather events such as prolonged heavy rainfall, storms, floods, and intense heat are becoming more complex and difficult to predict. In particular, in mountainous and complex terrain areas, sudden increases in rainfall have led to a higher frequency and severity of landslides, causing instability in road subgrades. In conditions with weak soils or untreated subgrades, the risk of settlement, sliding, and subgrade failure is high, potentially resulting in serious traffic accidents and damage to life and property.



Figure 1. Roadbed reinforcement anchor

Among the solutions for stabilizing roadbeds in mountainous areas, steel anchors are considered one of the

most suitable technologies for sections with deep excavation. Anchors are devices installed into the ground to transfer tensile forces into compressive forces within the upper soil/rock layers and the load-bearing soil stratum. This paper was developed based on a review of both domestic [1, 2, 3] and international standards [4] on anchors, as well as previous research results related to anchoring systems [5, 6, 7, 8].

2. Theoretical Basis for Stability Calculation

2.1. Finite Difference Method (FDM)

This is a numerical method used to solve partial differential equations through the following steps: the computational domain is discretized into a grid of polygonal cells, and the target variables are computed at the grid nodes. At each node, partial derivatives (or derivatives) are approximated using finite differences, resulting in algebraic equations [6].

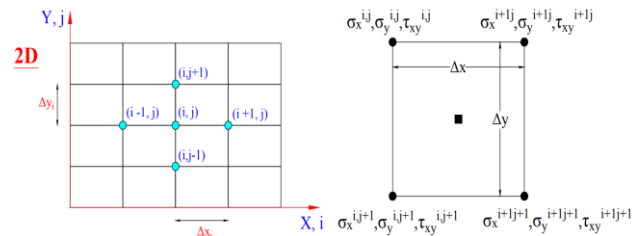


Figure 2. Rectangular Mesh and Finite Difference Grid for Calculation

By applying this process to all grid nodes, a system of linear equations is obtained, where the unknowns are the values of the studied variables at each node. This system, when combined with the equations representing boundary conditions, forms a complete system of N independent linear equations to solve for N unknowns.

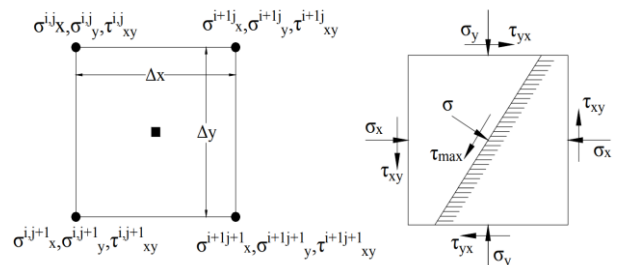


Figure 3. Shear Stress and Finite Difference Grid Cells

The method for determining slope stability using the Finite Difference Method (FDM) commonly applies the Strength Reduction Method, in which soil strength parameters such as cohesion and internal friction angle are simultaneously reduced according to the following equation:

$$C_{reduced} = \frac{c}{F}, \quad \tan\phi_{reduced} = \frac{\tan\phi}{F}$$

The maximum shear stress (τ_{max}) and the corresponding normal stress (σ) on this plane are determined using the following equations:

$$\left\{ \begin{array}{l} \tau_{max} = \frac{\sigma_1 - \sigma_2}{2} \\ \sigma = \frac{\sigma_1 + \sigma_2}{2} \end{array} \right\} \quad (1)$$

Where: σ_1 , σ_2 are the principal stress components, determined from the stress state in the orthogonal coordinate system:

$$\tau_{max} = \left[\left(\frac{\sigma_x^{(i,j)} + \sigma_x^{(i+1,j)} + \sigma_x^{(i+1,j+1)}}{4} - \frac{\sigma_y^{(i,j)} + \sigma_y^{(i+1,j)} + \sigma_y^{(i+1,j+1)}}{4} \right)^2 + \left(\frac{\tau_{xy}^{(i,j)} + \tau_{xy}^{(i+1,j)} + \tau_{xy}^{(i+1,j+1)}}{4} \right)^2 \right]^{0.5} \quad (2)$$

2.2. Base normal force

The normal force at the base of each slice (N) is a key variable in both the moment and force equilibrium safety factor equations. The magnitude of this normal force depends on the shear forces (X_L and X_R) acting on the slice, as illustrated in Figure 1 [9].

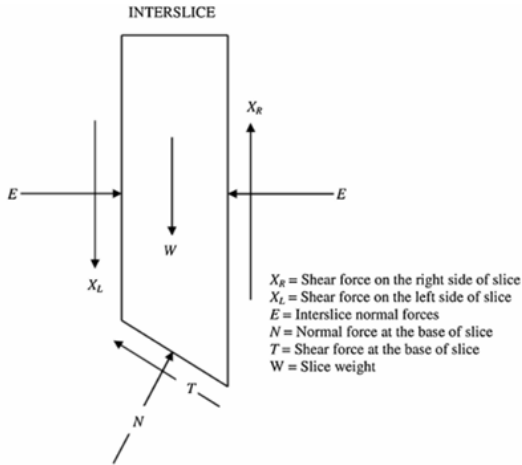


Figure 4. Forces acting on a single slice

The base normal force is calculated using the following equation:

$$N = \frac{W + (X_L - X_R) - \left(\frac{c' \beta \sin \alpha + u \beta \sin \alpha \tan \phi'}{F} \right)}{\cos \alpha + \frac{\sin \alpha \tan \phi'}{F}} \quad (3)$$

where: X_R is shear force on the right side of the slice, X_L is shear force on the left side of the slice, E is normal force between slices (inter-slice normal force), N is normal force at the base of the slice, T is shear force at the base of the slice, and W is weight of the slice.

2.3. Anchored Slope Stability Model

The anchored slope stability model incorporates the anchor forces' two main components: horizontal and vertical, considering the number of anchors, design load, pull-out capacity, grout-soil bond strength, anchor diameter, and length [5].

Formulating the global stability problem of an anchor-reinforced slope:

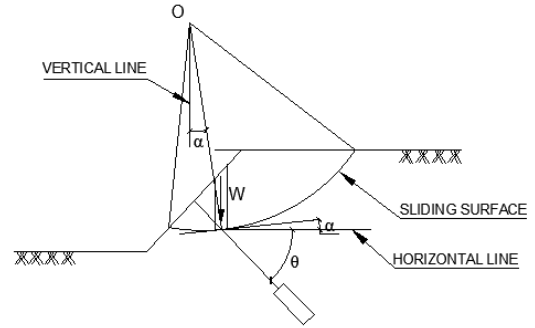


Figure 5. Method for stabilizing slopes using anchors

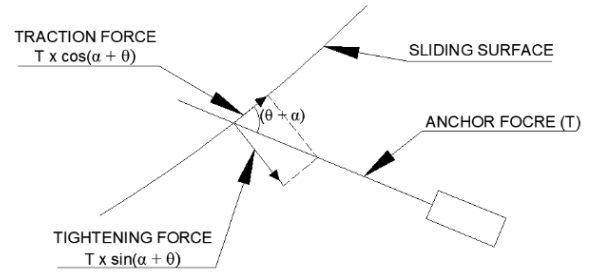


Figure 6. Two force components of the anchor system

$$F_{sp} = \frac{\sum_{i=1}^m T_{neo} + \sum_{i=1}^n c_i \Delta l_i + \tan \phi \sum_{i=1}^n (w_i \cos \alpha - u_i \Delta l_i)}{\sum_{i=1}^n (w_i \sin \alpha)} \quad (4)$$

$$T_{neo} = T_d [\sin(\alpha + \theta) \tan \phi + \cos(\alpha + \theta)] \quad (5)$$

Local stability analysis – Pullout resistance of anchor bulbs:

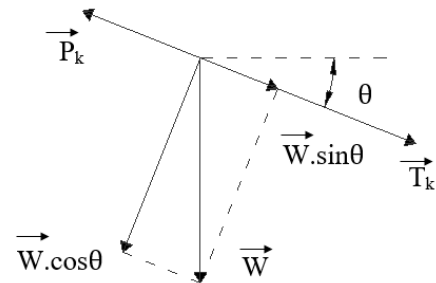


Figure 7. Force equilibrium in the local stability analysis

$$F_{sp} = \frac{T_k + W \sin \theta}{P_k} \quad (6)$$

$$T_k = \pi \cdot D \cdot L \cdot \tau \quad (7)$$

Where: F_{sp} is safety factor after anchoring reinforcement, θ is anchor inclination angle relative to the horizontal, m is Number of anchors, T_d is design tensile force per unit width, T_{anchor} is total force acting on a single anchor, P_k is

tensile force at the anchor head, T_k is pullout resistance of the anchor bulb, D is diameter of the anchor bulb, L is length of the anchor bulb, and τ is bond stress between soil and the anchor bulb.

Remark: Each calculation method has its own advantages and limitations. In this study, the finite element method is employed to assess the stability of the roadbed, using FLAC software as the supporting tool.

3. Optimization of Anchor Design

3.1. Research Objective

The study determines the optimal anchor inclination angles for a 21-meter-high excavated slope cross-section divided into three levels, with slope ratios of 1:0.5 and 1:0.75. In addition, a comparison is made to select the most effective reinforcement option between increasing the number of anchors and increasing the length of anchors [7].

3.2. Cross-section parameters and geological layers

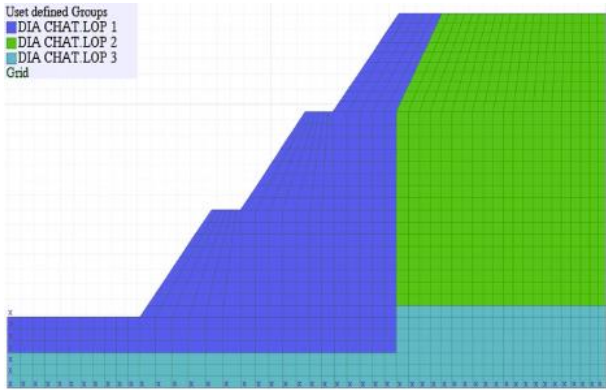


Figure 8. Geological model

Table 1. The physical and mechanical properties of the geological layers[5]

Parameters		Symbol					
		γ_{tn} (KN/m ³)	γ_{bh} (KN/m ³)	C (KN/m ²)	φ	θ	ψ
Geological Profile 1	Soil Layer 1	15,95	18,60	15	27°	0,35	0
	Soil Layer 2	26,09	26,09	4,0.10 ⁵	34°	0,10	0
	Soil Layer 3	26,09	26,09	4,25.10 ⁶	36°	0,10	0
Geological Profile 2	Soil Layer 1	15,95	18,60	15	27°	0,35	0
	Soil Layer 2	26,09	26,09	4,0.10 ⁴	34°	0,10	0
	Soil Layer 3	26,09	26,09	4,25.10 ⁴	36°	0,10	0
Geological Profile 3	Soil Layer 1	15,95	18,60	15	27°	0,35	0
	Soil Layer 2	22,00	22,00	1,8.10 ⁵	30°	0,25	0
	Soil Layer 3	26,09	26,09	4,25.10 ⁵	36°	0,25	0

The horizontal thickness of the geological layers measured from the slope surface, as shown in Figure 7, is as follows: Layer 1: from 3 m to 18 m; Layer 2: from 4 m to 19 m; Layer 3: from 19 m to 25 m.

3.3. Stability Check Without Anchors

Geological Profile 1 [1, 4, 7, 10]:

FLAC software is applied, and the calculated stability factor is $K = 1.055$; less than the required threshold $[K] = 1.2$.

After analysis, the minimum safety factor obtained for the existing slope condition is $K = 1.00 < [K] = 1.2$; indicating that the slope is unstable.



Figure 9. Critical slip surface

Geological Profile 2 [1, 4, 7, 10]:

FLAC software was applied, and the computed stability factor was $K = 1.072$, which is less than the required threshold $[K] = 1.2$.

After analysis, the minimum safety factor obtained for the existing slope condition is $K = 1.072 < [K] = 1.2$; indicating that the slope is unstable.



Figure 10. Critical slip surface

Geological Profile 3 [1, 4, 7, 10]:

FLAC software was applied, and the computed stability factor was $K = 1.057$, which is less than the required threshold $[K] = 1.2$.

After analysis, the minimum safety factor obtained for the existing slope condition is $K = 1.057 < [K] = 1.2$; indicating that the slope is unstable.



Figure 11. Critical slip surface

Legend:

Red: Minimal or no deformation – likely stable zone.

Orange–Yellow: Initial deformation – low to moderate level.

Green: Significant deformation – high load or potential failure zone.

Cyan–Blue: Maximum deformation – unstable or reinforcement required.

3.4. Determining Optimal Anchor Angle

Table 2. Anchor Parameters[5]

Parameters	Steel anchor	Unit
Diameter	Ø28	mm
Length	8,00	m
Quantity	9,00	pcs
Cross-sectional area	6,032E-4	m ²
Young's Modulus	2,01E11	Pa
Ultimate tensile strength	5,429E5	N

Table 3. Grout Parameters[5]

Parameters	Grout Material	Unit
Bond stiffness	3,01E9	N/m/m
Bond strength	8,756E5	N/m
Bond friction angle	30°	
Perimeter	0,113097	m

3.4.1. Optimal anchor angle for Geological Profile 1

To determine the most appropriate anchor inclination angle, in Case 1 (slope ratio 1:0.5), the study develops a model with 9 installed anchors, each with a length of 8.0 meters. Calculations are performed for various anchor angles, specifically: 20°, 25°, 30°, 35°, 40°, and 45°.

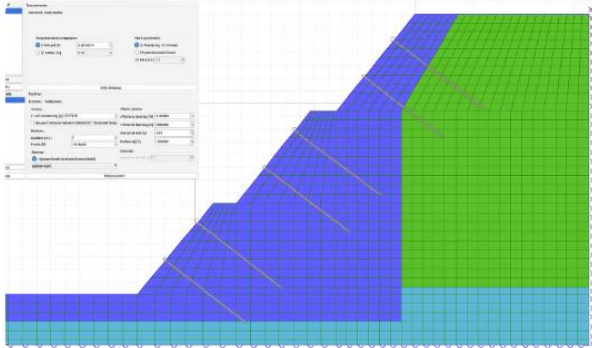


Figure 12. Anchors arranged at 40° with a slope of 1:0.75

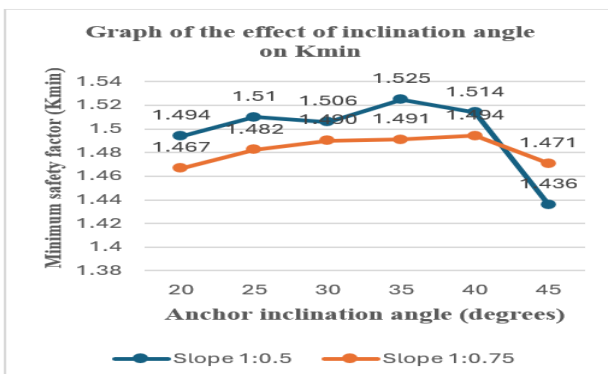


Figure 13. Chart comparing slope stability factors for various anchor inclination angles under geological condition 1

To determine the most suitable anchor inclination

angle, in Case 1 (slope ratio 1:0.75), a model was developed with 6 anchors, each 8.0 meters in length. Calculations were carried out for various anchor angles: 20°, 25°, 30°, 35°, 40°, and 45° [7, 8, 10].

From the chart above, Kmin reaches its maximum value when the anchor inclination is 35° for a 1:0.5 slope and 40° for a 1:0.75 slope.

3.4.2. Optimal anchor angle for Geological Profile 2

To determine the most appropriate anchor inclination angle (with respect to the horizontal plane), in Case 2 (slope ratio 1:0.5), a model was developed with 9 installed anchors, each 8.0 meters in length. Calculations were performed for anchor angles of 25°, 30°, 35°, 40°, 45°, and 50°.

To determine the most appropriate anchor inclination angle (relative to the horizontal plane), in Case 2 (slope ratio 1:0.75), a model was developed with 6 anchors, each 8.0 meters in length. Calculations were performed for anchor angles of 25°, 30°, 35°, 40°, 45°, and 50° [7, 8, 10].

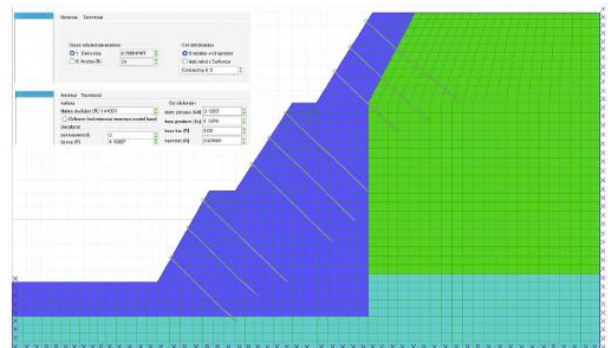


Figure 14. Anchors arranged at 45° with a slope of 1:0.5

From the above chart, it can be observed that Kmin reaches its maximum value when the anchor inclination angle is 45°.

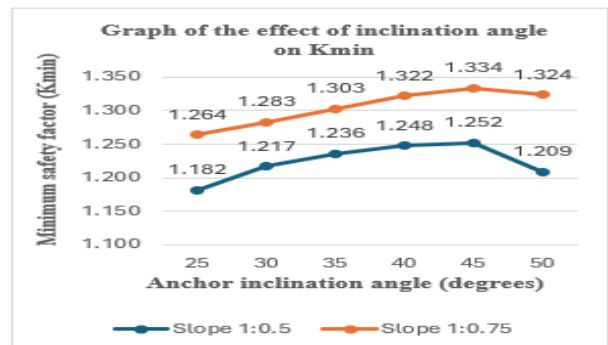


Figure 15. Comparison chart of slope stability factors for different anchor inclination cases under geological condition 2

3.4.3. Optimal anchor angle for Geological Profile 3

To determine the most appropriate anchor inclination angle, in Case 3 (slope ratio 1:0.5), a model was developed with 9 anchors, each 8.0 meters in length. Calculations were conducted for anchor angles of 20°, 25°, 30°, 35°, 40°, and 45°.

To determine the most appropriate anchor inclination angle, in Case 3 (slope ratio 1:0.75), a model was developed with 6 anchors, each 8.0 meters in length.

Calculations were carried out for anchor angles of 20°, 25°, 30°, 35°, 40°, and 45° [7, 8, 10].

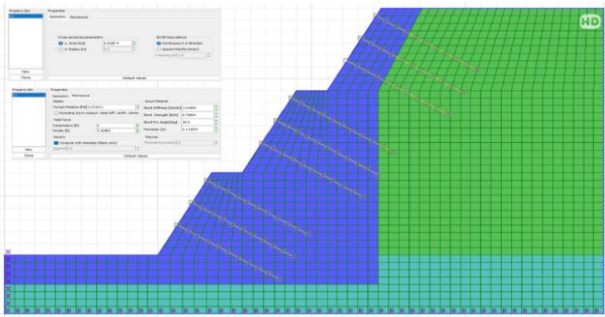


Figure 16. Anchors arranged at 30° with a slope of 1:0.5

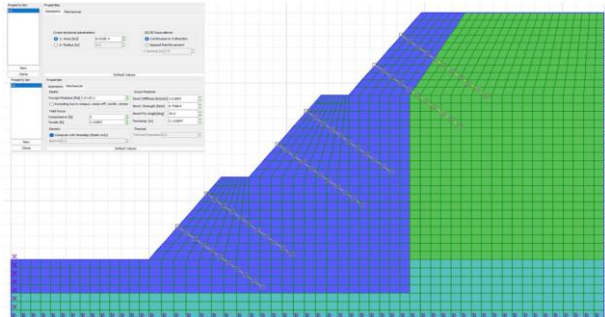


Figure 17. Anchors arranged at 35° with a slope of 1:0.75

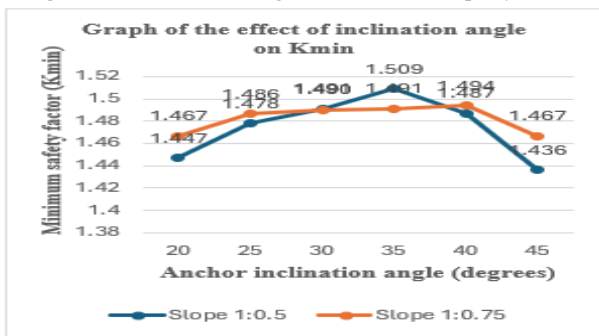


Figure 18. Comparison chart of slope stability factors for different anchor inclination cases under geological condition 3

From the chart above, Kmin reaches its maximum value when the anchor inclination is 30° for a 1:0.5 slope and 35° for a 1:0.75 slope.

Based on the optimal anchor inclination angles corresponding to the three geological conditions for the two slope ratios of 1:0.5 and 1:0.75, it can be seen that the optimal anchor angle lies within the range of 30° to 45°.

This result is also consistent with several domestic studies. For example, according to Prof. Vu Dinh Phung [11], the anchor inclination angle relative to the horizontal varies as follows: for cohesive soils, $\alpha = 5^\circ\text{--}25^\circ$; for cohesionless soils, $\alpha = 5^\circ\text{--}35^\circ$; and in the presence of groundwater, $\alpha = 10^\circ\text{--}45^\circ$. The study by Associate Professor Nguyen Hung Son [12] also indicates that the optimal anchor angle for flexible retaining walls is 35°.

3.5. Axial Force Distribution in Anchors

Corresponding to the optimal anchor angles, the axial force distribution in the anchor rods is shown in the following chart [7]:

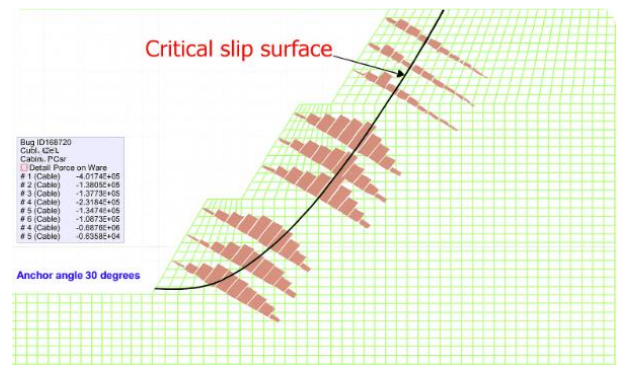


Figure 19. Critical slip surface of the slope

The critical slip surface of the slope was identified by connecting the points corresponding to the maximum axial forces along the anchors. These points represent the locations where the interaction between the anchors and the surrounding soil reaches its peak, indicating the potential failure path. Thus, the derived curve effectively defines the most critical slip surface governing the overall stability of the slope.

3.6. Comparative Analysis of Anchor Length and Quantity

Based on the results from the previous two sub-cases of Case 1, using 9 anchors of 8.0 m length, with an optimal inclination angle of 30° in one case and 45° in the other, the Author proposes to reduce the number of anchors to 6 while increasing the anchor length. The objective is to achieve the same factor of safety in both cases despite the reduced number of anchors.

Case 1:

Option 1: 9 anchor bars, length is 8.0m, anchor angle is 30°, Kmin = 1.52 [7].

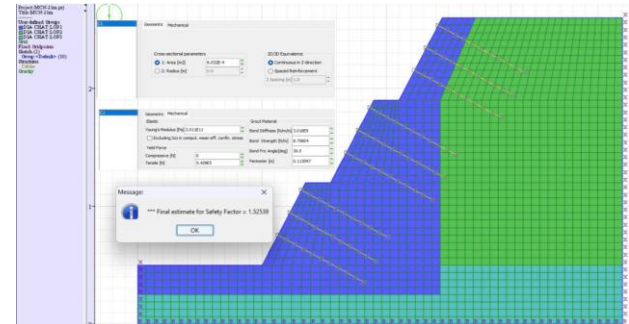


Figure 20. Layout of 9 anchors, each 8.0 m in length, inclined at 30°

Option 2: 6 anchor bars, each bar is 10.0m long. The angle of inclination of the anchor is 30°, Kmin = 1.43 [7].

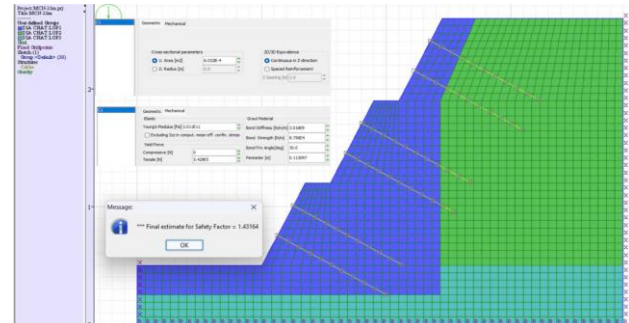


Figure 21. Layout of 6 anchors, each 10.0 m in length, inclined at 30°

Case 2:

Option 1: 9 anchor bars each 8.0m long, the angle of inclination of the anchor is 45° , $K_{min} = 1.25$ [7].

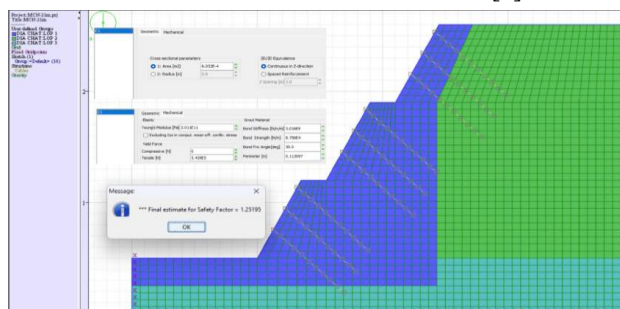


Figure 22. Layout of 9 anchors, each 8.0 m in length, inclined at 45°

Option 2: 6 anchor bars each 10.0m long, the angle of inclination of the anchor is 45° , $K_{min} = 1.21$ [7].

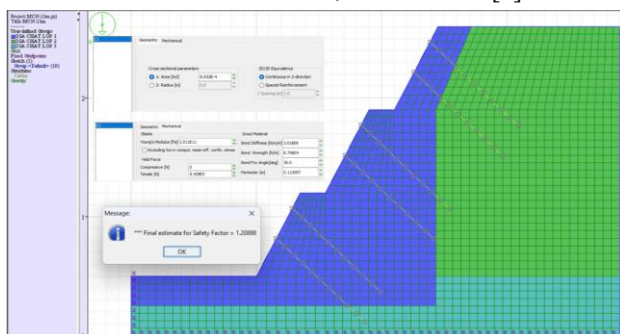


Figure 23. Layout of 6 anchors, each 10.0 m in length, inclined at 30°

The comparative analysis demonstrates that both anchor configurations 9 anchors of 8m and 6 anchors of 10m produce nearly identical safety factors, with differences of less than 5%. This indicates that extending anchor length can effectively compensate for a reduction in anchor quantity without compromising overall slope stability. Consequently, the configuration with 6 anchors of 10m length offers a more economical solution while maintaining equivalent performance. These findings highlight the importance of optimizing anchor geometry to achieve both technical efficiency and cost-effectiveness in slope reinforcement design.

4. Conclusion

The analysis indicates that the optimal anchor inclination depends on geological conditions. For

Geological Conditions 1, 2, and 3, the maximum safety factors were achieved at angles of 30° , 35° , and 45° , respectively, highlighting the need to adjust anchor inclination according to ground mechanical properties.

Consistent with previous studies suggesting a typical range of 20° – 35° (and up to 45° in specific cases), this study recommends an optimal range of 30° – 45° for reinforced roadbed slopes with gradients of 1:0.5–1:0.75.

Two layout strategies were analyzed: increasing anchor density with shorter lengths and reducing density with longer anchors. Results show similar safety factors in both cases, but the latter provides better economic efficiency while ensuring slope stability. Therefore, adopting fewer but longer anchors is recommended as a technically and economically optimal design solution.

REFERENCES

- [1] "Construction and acceptance of ground anchors used in transportation works", TCVN 8870:2011, 2011.
- [2] "Hydraulic works – Design anchors in soil and rock", TCVN 13808:2023, 2023.
- [3] Vietnam Road Administration, "Design, construction and acceptance of ground anchors using SEEE technology", TCCS 28: 2019/TCDBVN, 2019.
- [4] "Anchor in the ground", BS 8081:1989, 1989.
- [5] P. L. Le, "Research on reasonable distribution of tensile-compressive stress zones before reinforcing the slope of the excavated roadbed," The University of Danang, 2014.
- [6] C. T. Linh and P. K. Hai, "Calculation of Slope Reinforcement for Excavated Roadbed Using Prestressed Flexible Anchors Against Landslides and Rockfalls on the Hoang Van Thai Extension Road to Ba Na, Da Nang City", The University of Danang - Journal of Science and Technology, vol. 11, no. 96, pp. 103–109, 2015.
- [7] Itasca International, *FLAC 7.00 Update*, Itasca International, May 11, 2016. [Online]. Available: <https://www.itascainternational.com/software/downloads/flac-7-00-update>. [Accessed: Oct. 23, 2025]
- [8] C. T. Linh and L. P. Linh, "Study on the Stress and Strain Behavior of Slopes Reinforced with Different Types of Anchors," *Journal of Transport*, ISSN 2354-0818, no. 1, pp. 68–71, 2015.
- [9] C. T. Linh, "Research on distribution of tensile stress in anchors, reasonable length of prestressed anchor system by finite element method to stabilize collapse of slope of Ho Chi Minh road," Science and Technology Topic, code T04-15-77, 2015.
- [10] "Anti-slump works on highways – Survey and design requirements", TCVN 13346:2021, 2021.
- [11] V. D. Phung and SE Group Japan – SEC, "Draft technical guidelines for the design and construction of soil anchors" Vietnam, 2011.
- [12] N. H. Son and V. Q. Trung, "Optimal anchor arrangement for anchored retaining walls," *Journal of Construction Science and Technology-IBST*, pp. 1–4, 2011.